A Study of Strange Particles Produced in Neutrino Neutral Current Interactions in the NOMAD Experiment

NOMAD Collaboration

D. Naumov [f,*], A. Chukanov [f], E. Naumova [f], B. Popov [f,n],
P. Astier [n], D. Autiero [h], A. Baldisseri [r], M. Baldo-Ceolin [m],
M. Banner [n], G. Bassompierre [a], K. Benslama [i], N. Besson [r],
I. Bird [h,i], B. Blumenfeld [b], F. Bobisut [m], J. Bouchez [r], S. Boyd [t],
A. Bueno [c,x], S. Bunyatov [f], L. Camilleri [h], A. Cardini [j],
P.W. Cattaneo [o], V. Cavasinni [p], A. Cervera-Villanueva [h,v],
R. Challis [k], G. Collazuol [m], G. Conforto [h,u,1], C. Conta [o],
M. Contalbrigo [m], R. Cousins [j], D. Daniels [c], R. Das [c],
H. Degaudenzi [i], T. Del Prete [p], A. De Santo [h,p], T. Dignan [c],
L. Di Lella [h,2], E. do Couto e Silva [h], J. Dumarchez [n], M. Ellis [t],
G.J. Feldman [c], R. Ferrari [o], D. Ferrère [h], V. Flaminio [p],
M. Fraternali [o], J.-M. Gaillard [a], E. Gangler [h,n], A. Geiser [e,h],
D. Geppert [e], D. Gibin [m], S. Gninenko [h,ℓ], A. Godley [s],
J.-J. Gomez-Cadenas [h,v], J. Gosset [r], C. Gößling [e],
M. Gouanère [a], A. Grant [h], G. Graziani [g], A. Guglielmi [m],
C. Hagner [r], J. Hernando [v], T.M. Hong [c], D. Hubbard [c],
P. Hurst [c], N. Hyett [k], E. Iacopini [g], C. Joseph [i], F. Juget [i],
N. Kent [k], M. Kirsanov [ℓ], O. Klimov [f], J. Kokkonen [h],
A. Kovzelev [ℓ,o], A. Krasnoperov [f,a], S. Lacaprara [m],
C. Lachaud [n], B. Lakić [w], A. Lanza [o], L. La Rotonda [d],
M. Laveder [m], A. Letessier-Selvon [n], J.-M. Levy [n], L. Linssen [h],
A. Ljubičić [w], J. Long [b], A. Lupi [g], V. Lyubushkin [f],
A. Marchionni [g], F. Martelli [u], X. Méchain [r], J.-P. Mendiburu [a],
J.-P. Meyer [r], M. Mezzetto [m], S.R. Mishra [c,s], G.F. Moorhead [k],
P. Nédélec [a], Yu. Nefedov [f], C. Nguyen-Mau [i], D. Orestano [q],
F. Pastore [q], L.S. Peak [t], E. Pennacchio [u], H. Pessard [a],
R. Petti [h,o], A. Placci [h], G. Polesello [o], D. Pollmann [e],
A. Polyarush [ℓ], C. Poulsen [k], L. Rebuffi [m], J. Rico [x],

arXiv:hep-ex/0409037v1 14 Sep 2004

P. Riemann[e], C. Roda[h,p], A. Rubbia[h,x], F. Salvatore[o],
K. Schahmaneche[n], B. Schmidt[e,h], T. Schmidt[e], A. Sconza[m],
M. Sevior[k], D. Shih[c], D. Sillou[a], F.J.P. Soler[h,t], G. Sozzi[i],
D. Steele[b,i], U. Stiegler[h], M. Stipčević[w], Th. Stolarczyk[r],
M. Tareb-Reyes[i], G.N. Taylor[k], V. Tereshchenko[f],
A. Toropin[ℓ], A.-M. Touchard[n], S.N. Tovey[h,k], M.-T. Tran[i],
E. Tsesmelis[h], J. Ulrichs[t], L. Vacavant[i], M. Valdata-Nappi[d,3],
V. Valuev[j,f], F. Vannucci[n], K.E. Varvell[t], M. Veltri[u],
V. Vercesi[o], G. Vidal-Sitjes[h], J.-M. Vieira[i], T. Vinogradova[j],
F.V. Weber[c,h], T. Weisse[e], F.F. Wilson[h], L.J. Winton[k],
B.D. Yabsley[t], H. Zaccone[r], K. Zuber[e], P. Zuccon[m]

[a]*LAPP, Annecy, France*
[b]*Johns Hopkins Univ., Baltimore, MD, USA*
[c]*Harvard Univ., Cambridge, MA, USA*
[d]*Univ. of Calabria and INFN, Cosenza, Italy*
[e]*Dortmund Univ., Dortmund, Germany*
[f]*JINR, Dubna, Russia*
[g]*Univ. of Florence and INFN, Florence, Italy*
[h]*CERN, Geneva, Switzerland*
[i]*University of Lausanne, Lausanne, Switzerland*
[j]*UCLA, Los Angeles, CA, USA*
[k]*University of Melbourne, Melbourne, Australia*
[ℓ]*Inst. for Nuclear Research, INR Moscow, Russia*
[m]*Univ. of Padova and INFN, Padova, Italy*
[n]*LPNHE, Univ. of Paris VI and VII, Paris, France*
[o]*Univ. of Pavia and INFN, Pavia, Italy*
[p]*Univ. of Pisa and INFN, Pisa, Italy*
[q]*Roma Tre University and INFN, Rome, Italy*
[r]*DAPNIA, CEA Saclay, France*
[s]*Univ. of South Carolina, Columbia, SC, USA*
[t]*Univ. of Sydney, Sydney, Australia*
[u]*Univ. of Urbino, Urbino, and INFN Florence, Italy*
[v]*IFIC, Valencia, Spain*
[w]*Rudjer Bošković Institute, Zagreb, Croatia*
[x]*ETH Zürich, Zürich, Switzerland*

Abstract

Results of a detailed study of strange particle production in neutrino neutral current interactions are presented using the data from the NOMAD experiment. Integral yields of neutral strange particles (K_s^0, Λ, $\bar{\Lambda}$) have been measured. Decays of resonances and heavy hyperons with an identified K_s^0 or Λ in the final state have been analyzed. Clear signals corresponding to $K^{\star\pm}$ and $\Sigma(1385)^{\pm}$ have been observed. First results on the measurements of the Λ polarization in neutral current interactions have been obtained.

1 Introduction

A study of strange particle production in neutrino neutral current (NC) interactions is important, especially taking into account the fact that strange particle production in ν NC is different from neutrino charged current (CC) interactions at the quark level. For example, NC interactions can produce a leading down quark, a leading up quark and even a leading strange quark, whereas CC interactions are a source of leading up and charm quarks only.

A previous study of neutral strange particle production in ν_μ NC interactions has been performed by the E632 Collaboration [1] using the Fermilab 15-foot bubble chamber exposed to the Tevatron (anti)neutrino beam with an average energy of $\langle E_{\nu(\bar{\nu})} \rangle = 150$ (110) GeV. The selected V^0 sample in NC events is presented in Table 1, and amounts to 81 events only. The $z = E_{V^0}/E_{had}$ distributions have also been published [1].

In our recent articles [2,3] we reported results on the measurements of the polarization of Λ and $\bar{\Lambda}$ hyperons in ν_μ CC interactions. This is an active field of research intimately related to the proton spin puzzle, spin transfer mechanisms and fragmentation processes. Following our publication [2] the longitudinal Λ polarization was investigated in much detail in a theoretical paper [4] in which agreement was found between the tuned polarized intrinsic model predictions and NOMAD results. It is a natural step to confront the predictions of this model for the longitudinal polarization of Λ hyperons produced in neutrino nucleon neutral current deep inelastic scattering (DIS) with

* Corresponding author.
  Email address: `naumov@nusun.jinr.ru` (D. Naumov).
[1] Deceased
[2] Now at Scuola Normale Superiore, Pisa, Italy
[3] Now at Univ. of Perugia and INFN, Perugia, Italy

Table 1

The number of reconstructed V^0 events and the corrected V^0 rates (yield per event) in ν_μ NC interactions for different cuts on the visible hadronic energy, p_{had}^{vis}, as measured in the E632 experiment (from [1]).

	$p_{had}^{vis} > 10\ GeV$	$p_{had}^{vis} > 25\ GeV$
NC events	670	437
Observed K^0	48	28
Observed Λ	29	19
Observed $\bar{\Lambda}$	4	2
Corrected K^0 rate	0.344 ± 0.065	0.322 ± 0.073
Corrected Λ rate	0.111 ± 0.025	0.113 ± 0.030

experimental measurements. The large statistics of the NOMAD data (about 300K reconstructed NC events) provides a tool to perform such a study.
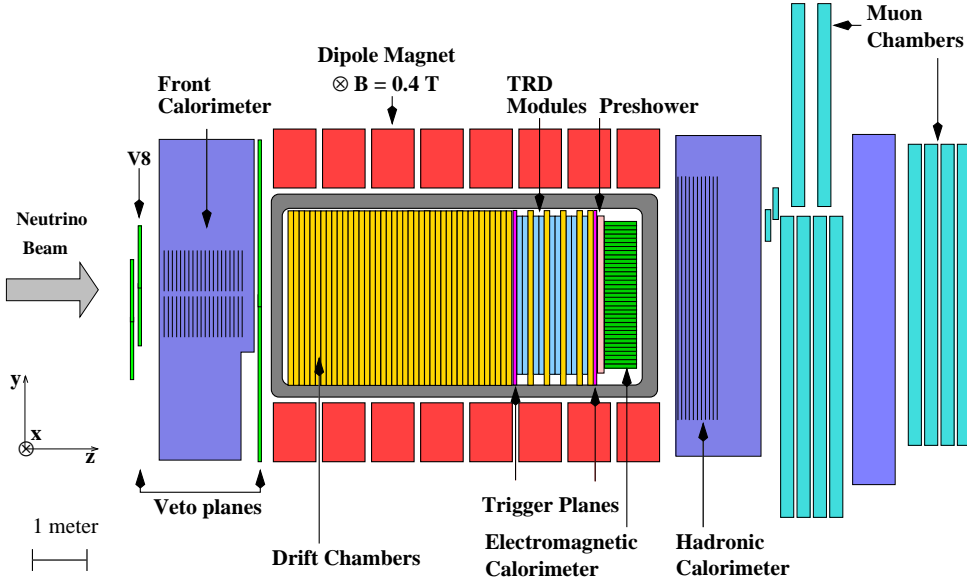

Fig. 1. A sideview of the NOMAD detector.

The NOMAD detector [5] (see Fig. 1) consisted of an active target of 44 drift chambers, with a total fiducial mass of 2.7 tons, located in a 0.4 Tesla dipole magnetic field. The coordinate system used in the NOMAD experiment is shown in Fig. 1. The drift chambers [6], made of low Z material (mainly carbon) served the double role of a (nearly isoscalar) target for neutrino inter-actions and of the tracking medium. The average density of the drift chamber volume was 0.1 g/cm^3. These drift chambers provided an overall efficiency for charged track reconstruction of better than 95% and a momentum resolution of approximately 3.5% in the momentum range of interest (less than 10 GeV/c). Reconstructed tracks were used to determine the event topology (the assign-

ment of tracks to vertices), to reconstruct the vertex position and the track parameters at each vertex and, finally, to identify the vertex type (primary, secondary, V^0, etc.). The vertex position resolution is 600 μm, 90 μm and 860 μm in x, y and z respectively. A transition radiation detector [7] placed at the end of the active target was used for electron identification. A lead-glass electromagnetic calorimeter [8] located downstream of the tracking region provided an energy resolution of $3.2\%/\sqrt{E[\mathrm{GeV}]}\oplus1\%$ for electromagnetic showers and was essential to measure the total energy flow in neutrino interactions. In addition, an iron absorber and a set of muon chambers located after the electromagnetic calorimeter were used for muon identification, providing a muon detection efficiency of 97% for momenta greater than 5 GeV/c.

The main characteristics of the neutrino beam [9] are given in Table 2.

Table 2
The CERN SPS neutrino beam composition [9].

Neutrino	Flux		CC interactions in NOMAD	
flavours	$< E_\nu >$ [GeV]	rel.abund.	$< E_\nu >$ [GeV]	rel.abund.
ν_μ	24.3	1	47.5	1
$\bar{\nu}_\mu$	17.2	0.0678	42.0	0.024
ν_e	36.4	0.0102	58.2	0.015
$\bar{\nu}_e$	27.6	0.0027	50.9	0.0015

Whenever possible the NOMAD data are compared to the results of a Monte Carlo (MC) simulation based on LEPTO 6.1 [10] and JETSET 7.4 [11] generators for neutrino interactions and on a GEANT [12] based program for the detector response. The relevant JETSET parameters have been tuned in order to reproduce the yields of all hadrons, including strange particles, as measured in ν_μ CC interactions in NOMAD [13]. A detailed paper devoted to the NOMAD MC tuning will be the subject of a forthcoming publication. To define the parton content of the nucleon for the cross-section calculation we have used the parton density functions parametrized in [14].

This article is organized as follows. The event selection criteria and a special algorithm developed for the identification of neutrino NC interactions are described in Sec. 2. The production yields of neutral strange particles (K_s^0, Λ and $\bar{\Lambda}$) are presented in Sec. 3, while yields of heavier resonances ($K^{\star\pm}$ and $\Sigma(1385)^{\pm}$) are reported in Sec. 4. A measurement of the Λ polarization vector is presented in Sec. 5. Finally, we summarize our results, compare them to the measurements in the ν_μ CC event sample and present our conclusions in Sec. 6.

2 Identification of neutrino NC interactions

In this section we describe the selection procedure for NC DIS events. An event with no *identified muon* is considered as a candidate for a NC interaction. However, such a simplified identification would lead to a considerable contamination from neutrino charged current events with *a reconstructed* muon which was *not identified* as a muon by the reconstruction algorithm based on the information from the muon chambers. We estimate such a contribution from ν_μ CC events with the help of the MC simulation to be about 30% of NC candidates. However, the difference in kinematic properties of NC and CC events can be used to discriminate between these two event categories. For this purpose we apply an identification of NC events which was used in [15] and consists of two main steps:

(1) Muon tagging, finding the negatively charged track most likely to be a muon, based on the topology of the event.
(2) CC rejection, using the likelihood based on event kinematics that the candidate muon originates indeed from a ν_μ CC interaction.

To tune our identification algorithm we use two MC subsamples (CC and NC) each corresponding to one half of the total MC statistics (well over 10^6 events) and we require that:

(1) There is no identified negatively charged muon in the event.
(2) The primary vertex of the event is in the restricted fiducial volume: $|X, Y| < 120$ cm, 5 cm $< Z < 350$ cm.
(3) There should be at least two charged tracks at the primary vertex in the event of which at least one must be negative.
(4) The visible hadronic energy should be larger than 3 GeV.

The actual NC selection efficiency and background contamination are then determined using the second halves of the MC event samples.

2.1 Muon Tagging

In what follows we describe our procedure to tag the primary muon produced at the charged current vertex. The kinematic variables used in this procedure are defined in Fig. 2. We have found that the following three variables provide the best discrimination between the true primary μ^- and any other negatively charged track from the hadronic jet:

(1) $\theta_{\nu l}$ - the angle between the track and the incoming neutrino direction (Z axis),
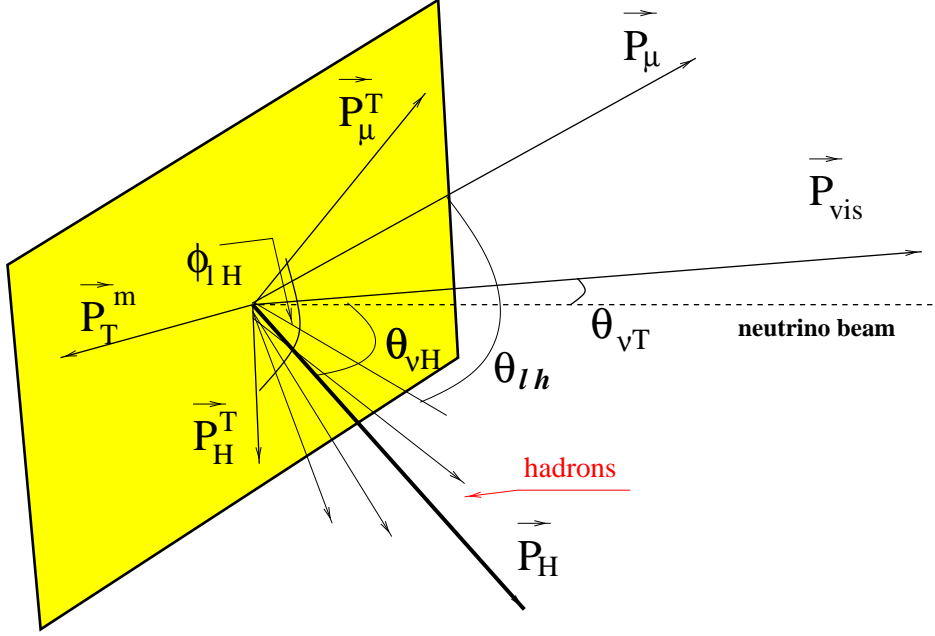
Fig. 2. Definition of kinematic variables used for the event tagging. The incoming neutrino direction is along the Z axis shown by the dashed line.

(2) p_T^l - the transverse momentum of the track with respect to the incoming neutrino direction,

(3) $R_{Q_T} = \langle Q_T^2 \rangle_H / \langle Q_T^2 \rangle_T$, where:

$$\langle Q_T^2 \rangle_H = \frac{1}{n-1} \sum_{j \neq i} Q_T^2(j),$$

$$\langle Q_T^2 \rangle_T = \frac{1}{n} \sum_j Q_T^2(j),$$

$$\mathbf{Q_T} = \mathbf{p}_i - \mathbf{p}_{\text{vis}} \frac{\mathbf{p}_i \cdot \mathbf{p}_{\text{vis}}}{\mathbf{p}_{\text{vis}}^2},$$

$\mathbf{p}_i$ is the momentum of the i-th track (assumed to be the candidate muon), and $\mathbf{p}_{\text{vis}}$ is the total momentum of the event, and n is the total number of tracks in the event.

As one can see from Fig. 3 the distributions of these variables in CC events with an unidentified muon are quite different if the i-th track is the true muon track or, instead, another negative primary track belonging to the hadronic system. The tagging algorithm is based on the following three-dimensional likelihood function:

$$\mathcal{L}^\mu = [\theta_{\nu l}, p_T^l, R_{Q_T}] \tag{1}$$

where the square brackets denote the correlations among the variables. A likelihood ratio, $\ln \lambda^\mu$, is built from ν_μ CC events with unidentified muons as the ratio of $\mathcal{L}^\mu$ for the true muon and for other negative tracks. We tag as candidate muon the primary negative track with the largest value of $\ln \lambda^\mu$. This
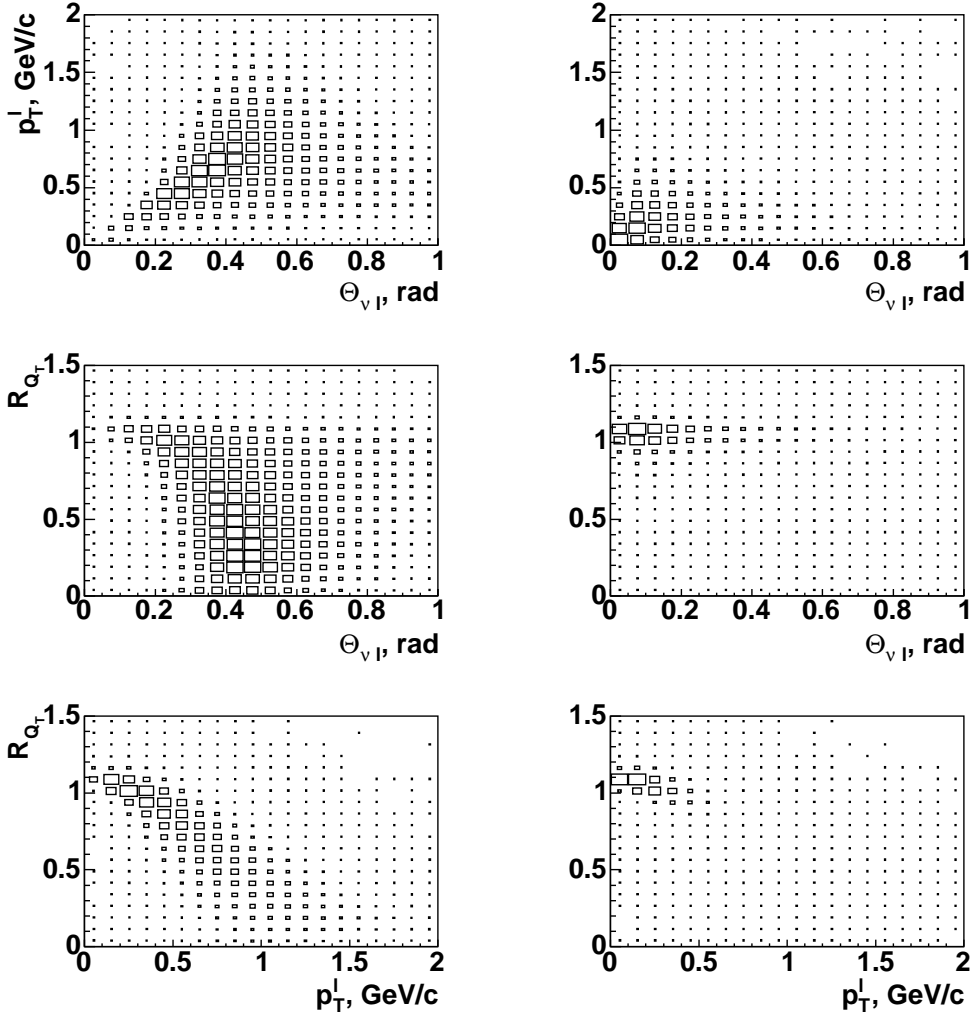
7

Fig. 3. Correlations between the kinematic variables θ^l_ν, P^l_T and R_Q for reconstructed but not identified muons (left plots) and for negatively charged primary hadrons (right plots) in ν_μ CC events.

procedure correctly identifies 86% of μ^- in ν_μ CC events with no identified muon, and 71% of e^- in ν_e CC events as well. Thus the muon tagging procedure can also be applied for the kinematical identification of primary electrons from ν_e CC events.

2.2 CC Event Rejection

The requirement of a tagged muon to be a track with maximum $\ln \lambda^\mu$ always provides us with a muon candidate, even in the case of NC events. However, it is possible to discriminate between NC and CC events using a multi-dimensional likelihood function which exploits the full event kinemat-

8

ics:

$$\mathcal{L}_6^{\mathrm{NC}} = [[[\theta_{\nu H}, \theta_{\nu T}], \theta_{lh_i}, Q_T], p_T^m, \phi_{lH}] \qquad (2)$$

where:

- $\theta_{\nu H}$ is the angle between the momentum of the hadronic system and the incident neutrino direction;
- $\theta_{\nu T}$ is the angle between the total visible momentum and the incident neutrino direction;
- θ_{lh_i} is the minimum opening angle between any primary track and the muon candidate;
- p_T^m is the missing transverse momentum;
- ϕ_{lH} is the azimuthal angle between the muon candidate and the hadronic system.

Some of the correlations among the kinematic variables used to build $\mathcal{L}_6^{\mathrm{NC}}$ are shown in Fig. 4 for true muons in ν_μ CC events with unidentified muons, and for the primary negative track with the largest value of $\ln \lambda^\mu$ in NC events. A likelihood ratio, $\ln \lambda_6^{\mathrm{NC}}$, is built as the ratio of the $\mathcal{L}_6^{\mathrm{NC}}$ function for the negative track tagged as the muon candidate in NC events, and for the true muon in ν_μ CC events with unidentified muons. All events with $\ln \lambda_6^{\mathrm{NC}} < 0.5$ are classified as CC interactions and rejected.

As a cross-check, we also use a different likelihood which depends on three variables only:

$$\mathcal{L}_3^{\mathrm{NC}} = [p_T{}^l, \rho, R_{Q_T}] \qquad (3)$$

where

$$\rho = \frac{p_T{}^l}{p_T{}^l + p_T{}^m}.$$

2.3 Efficiency and Purity

The NC identification procedure applied to both real and simulated events greatly reduces the contamination of charged current events with leading leptons not identified by the corresponding subdetectors, while keeping more than 60% of the useful signal.

In order to estimate the final purity of the ν NC sample in the data we processed in addition small samples of $\bar{\nu}_\mu$ CC, ν_e CC and $\bar{\nu}_e$ CC events through the same code. The final ν NC purity is computed as:

$$Purity = \frac{\sum_\alpha f_\alpha \epsilon(\alpha NC \to NC)}{\sum_{\alpha = \nu_\mu, \bar{\nu}_\mu, \nu_e, \bar{\nu}_e} f_\alpha \left(\frac{\sigma_{\alpha CC}}{\sigma_{\alpha NC}} \epsilon(\alpha CC \to NC) + \epsilon(\alpha NC \to NC) \right)},$$
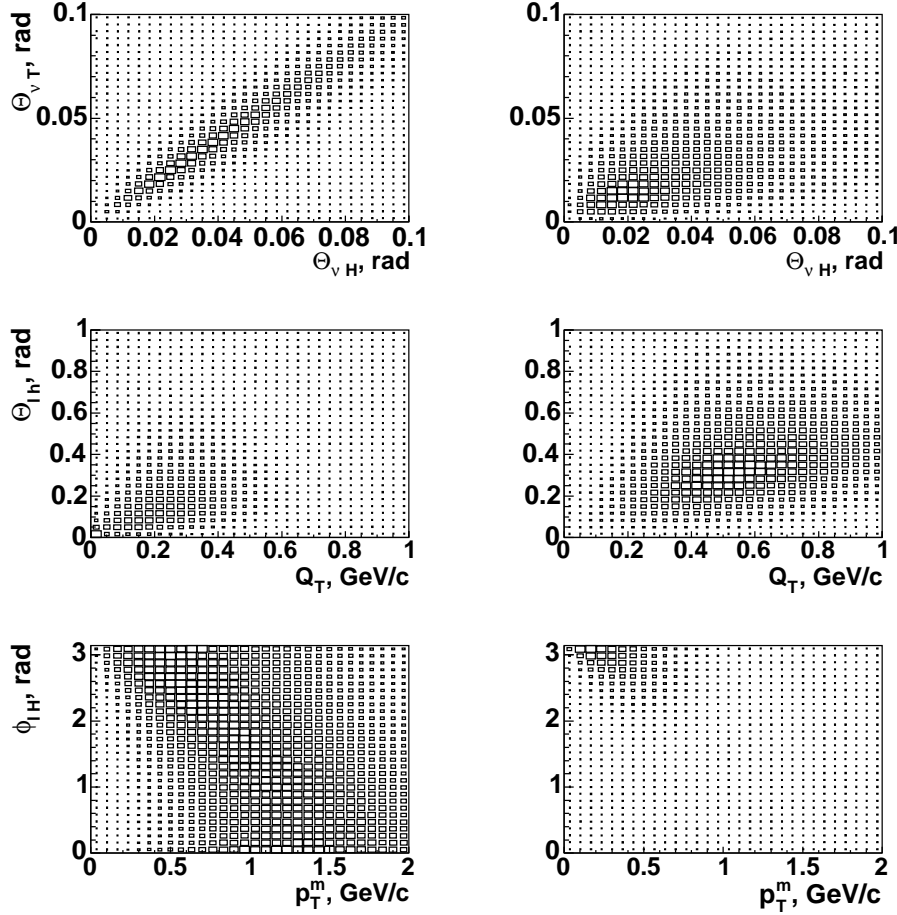
9

Fig. 4. Correlations among kinematic variables used to construct $\mathcal{L}_6^{\text{NC}}$ for negatively charged tracks with the maximal $\ln \lambda^\mu$ in ν_μ NC events (left plots) and for true muons in ν_μ CC events (right plots).

where f_α describe the beam composition (presented in Table 2) of $\bar{\nu}_\mu$, ν_e and $\bar{\nu}_e$ relative to the ν_μ component, $\sigma_{\alpha CC}$ and $\sigma_{\alpha NC}$ stand for the corresponding CC and NC cross-sections, and $\epsilon(\alpha CC(NC) \to NC)$ is the efficiency for the beam component α interacting via CC (NC) to be identified as NC signal. We assume that $\epsilon(\alpha NC \to NC)$ are all equal. The final purity and efficiency of the NC sample identified with $\ln \lambda_6^{\text{NC}}$ are displayed in Fig. 5 as a function of the cut on $\ln \lambda_6^{\text{NC}}$. The use of $\ln \lambda_3^{\text{NC}}$ as a cross-check gives a consistent number of NC events identified in the data, thus confirming our NC identification procedure.

In what follows we present our results with the $\ln \lambda_6^{\text{NC}}$ identification, since for a given ν NC efficiency $\ln \lambda_6^{\text{NC}}$ provides a better rejection of $\bar{\nu}_\mu$, ν_e and $\bar{\nu}_e$ CC events.

A sample of 226681 ν NC events is selected in the data with purity of 92% using the cut $\ln \lambda_6^{\text{NC}} > 0.5$. The ν_μ NC events being the dominating component
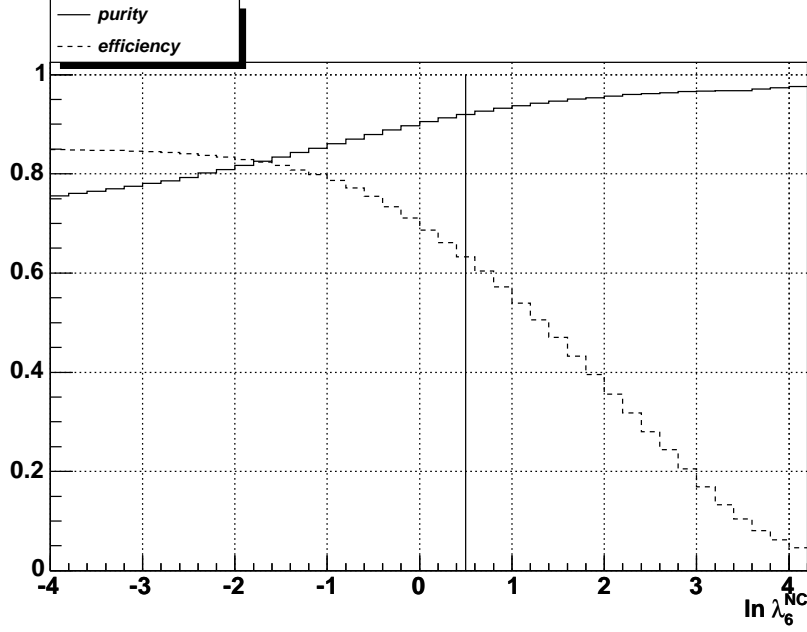
Fig. 5. Efficiency and purity of the NC identification as a function of a cut on the $\ln \lambda_6^{\mathrm{NC}}$. The final cut used is also shown.

of the final ν NC sample is selected with 62.7% efficiency.

Fig. 6 shows a comparison between the data and MC (normalized to the number of events in the data taking into account the actual beam composition) as a function of the $\ln \lambda_6^{\mathrm{NC}}$. These distributions can be seen to be in good agreement.

3 Production of neutral strange particles

We apply the V^0 identification algorithm developed for the CC event sample in [2] to identify neutral strange particles (Λ, K_s^0 and $\bar{\Lambda}$) in ν_μ NC sample. We find values for efficiencies and purities of the V^0 identification algorithm similar to those observed in the CC sample.

The numbers of neutral strange particles observed in the data with their identification purities are summarized in Table 3. This is a considerable improvement in statistics over the previously published data [1].

Fig. 7 shows the invariant mass distributions of two charged tracks from a V^0 vertex identified as K_s^0 and Λ in the data. The mean values of these distributions agree well with the PDG world averages [16] for K_s^0 and Λ masses respectively. The corresponding experimental resolutions are about 11 MeV/c^2 for $\mathrm{K}_s^0 \to \pi^+\pi^-$, and 4 MeV/$c^2$ for both $\Lambda \to \mathrm{p}\pi^-$ and $\bar{\Lambda} \to \bar{\mathrm{p}}\pi^+$.
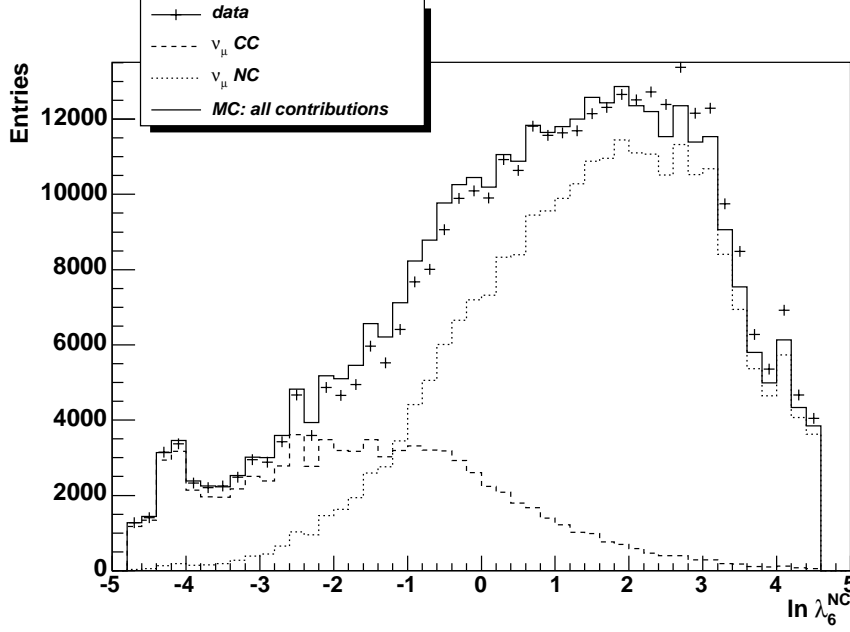
11

Fig. 6. Likelihood ratio $\ln \lambda_6^{\mathrm{NC}}$ distributions in the data (points) and in the MC (histogram) normalized to the number of events in the data taking into account the actual beam composition. The main contributions from ν_μ CC and ν_μ NC simulated events are shown separately.

Table 3

Number of V^0's in the data and their identification purities in NC interactions

#	DATA	Purity
$N(\mathrm{K}_{\mathrm{s}}^0)$	3691	97%
$N(\Lambda)$	1619	94%
$N(\bar{\Lambda})$	146	82%

The integral yields of neutral strange particles per neutrino interaction have been measured using the same approach as the one developed for the CC event sample [13]. The results are presented in Table 4. We find agreement at the level of 12% or better between data and the MC tuned on strange particle production in CC events. This has to be compared with the factor of two overestimation of strange particle yields in NC events by the MC with the default JETSET parameters [11].

It is interesting to compare the measured yields of neutral strange particles in NC interactions with those in ν_μ CC events. For such a comparison we applied the same kinematic criteria to CC events (except for the $Q^2 > 0.8$ GeV^2 cut applied for the CC sample and not applied for NC events) and obtained the yields summarized in Table 5. We emphasize the excellent agreement of production yields of strange particles between the data and MC CC samples
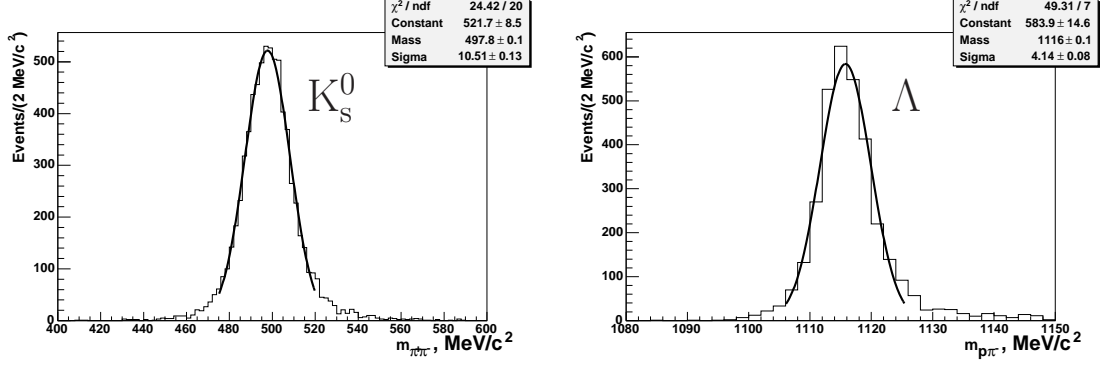
12

Fig. 7. Invariant mass distributions of two charged tracks from a V^0 vertex identified as K_s^0 (left) and Λ (right) in ν NC samples in data.

Table 4

Integral yields of V^0's in NC interactions in both the data and MC simulation. Only statistical errors are shown.

V^0 Type	$\mathcal{T}_{V^0}$ DATA	$\mathcal{T}_{V^0}$ MC	$\mathcal{T}_{V^0}^{MC}/\mathcal{T}_{V^0}^{DATA}$
Λ	$(5.16 \pm 0.14)\%$	$(5.79 \pm 0.02)\%$	1.12 ± 0.03
K_s^0	$(8.62 \pm 0.15)\%$	$(8.46 \pm 0.03)\%$	0.98 ± 0.02
$\bar{\Lambda}$	$(0.43 \pm 0.04)\%$	$(0.44 \pm 0.01)\%$	1.02 ± 0.11

obtained as a result of the MC tuning. From Tables 4 and 5 we conclude that the production yields of neutral strange particles in CC and NC events agree within a few percent.

We find a consistency between neutral strange particles production yields measured with our default cut $\ln \lambda_6^{NC} > 0.5$ and with the harder cut $\ln \lambda_6^{NC} > 3$. Varying the V^0 selection criteria [2] as well as the NC identification cut within reasonable limits we have estimated the systematic uncertainties on the V^0 production yields in neutrino NC interactions: 0.09 for Λ, 0.11 for K_s^0 and 0.03 for $\bar{\Lambda}$.

Table 5

Integral yields of V^0's in ν_μ CC interactions in both the data and MC simulation. Only statistical errors are shown.

V^0 Type	$\mathcal{T}_{V^0}$ DATA	$\mathcal{T}_{V^0}$ MC	$\mathcal{T}_{V^0}^{MC}/\mathcal{T}_{V^0}^{DATA}$
Λ	$(5.55 \pm 0.08)\%$	$(5.52 \pm 0.02)\%$	0.99 ± 0.02
K_s^0	$(8.54 \pm 0.08)\%$	$(8.51 \pm 0.02)\%$	1.00 ± 0.01
$\bar{\Lambda}$	$(0.43 \pm 0.02)\%$	$(0.46 \pm 0.01)\%$	1.05 ± 0.06

13

The dependence of the yields of K_s^0's, Λ's and $\bar{\Lambda}$'s in events in the data on the total hadronic energy E_{had} is shown in Fig. 8. As expected, the yields increase as a function of E_{had}.

We notice a reasonable agreement between NOMAD and E632 [1] measurements of neutral strange particles production rates.
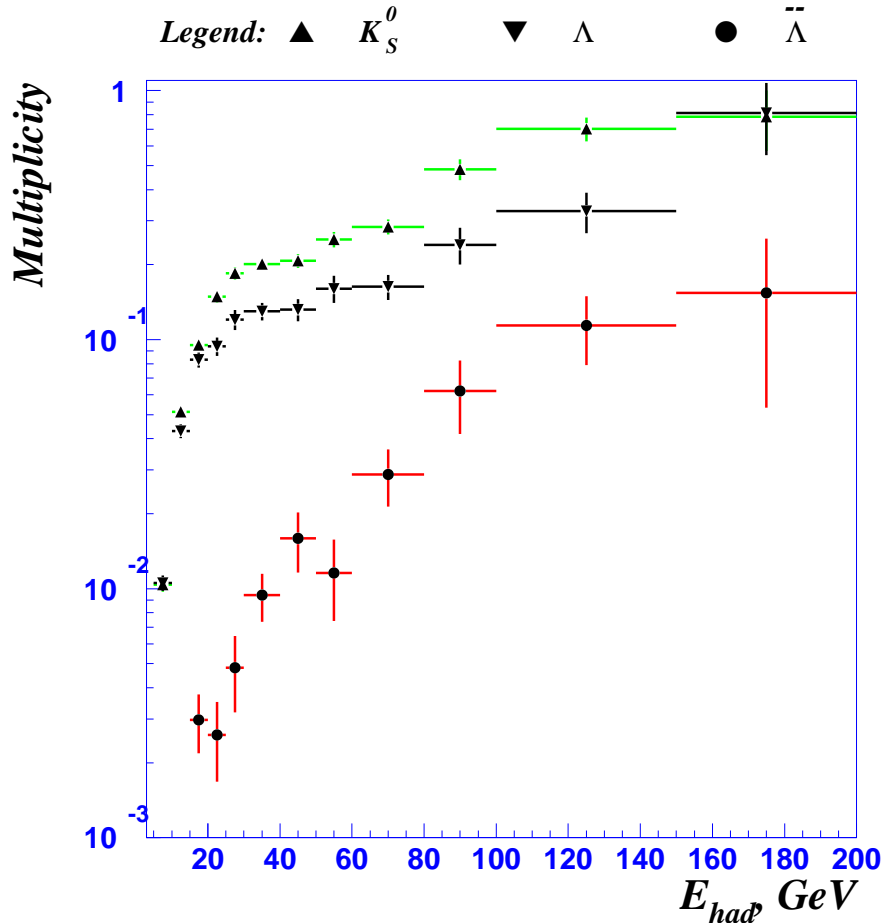

Fig. 8. *Dependence of the yields of* K_s^0*'s,* Λ*'s and* $\bar{\Lambda}$*'s on the total hadronic energy in the NC data sample.*

The distributions of the reconstructed $z = E_{V^0}/E_{had}$ variable for identified K_s^0's (left plot), Λ's (middle plot) and $\bar{\Lambda}$'s (right plot) in NC events are shown in Fig. 9 for both data and MC samples. There is an agreement between data and MC except for the K_s^0 case.

4 Study of heavier strange particles and resonances

We have studied the invariant mass distributions for $(K_s^0 \pi^{\pm})$ and $(\Lambda \pi^{\pm})$ combinations. The procedure used for the signal extraction is the one developed
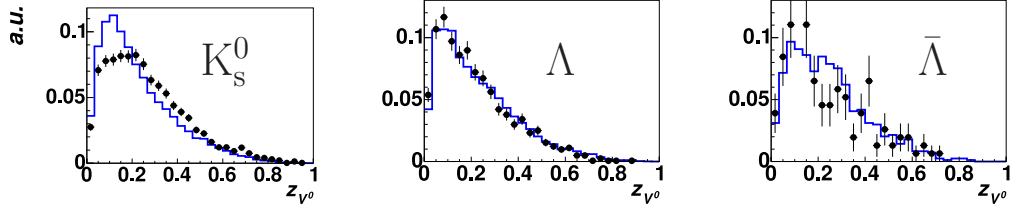
Fig. 9. Reconstructed z-distributions for identified K_s^0's (left plot), Λ's (middle plot) and $\bar{\Lambda}$'s (right plot) in ν NC samples both in the data (points with error bars) and in the MC (histogram).

for the ν_μ CC sample [13]. Clear signals corresponding to $K^{\star\pm}$ (see Fig. 10) and $\Sigma(1385)^\pm$ (see Fig. 11) have been observed. The results for the fraction of K_s^0 produced via $K^{\star\pm}$, $f_{K^\star} = (K^{\star\pm} \to K_s^0 \pi^\pm)/K_s^0$ are presented in Table 6. Similarly, the results for the fraction of Λ produced via $\Sigma(1385)^\pm$ decays, $f_{\Sigma^\star} = (\Sigma(1385)^\pm \to \Lambda\pi^\pm)/\Lambda$ are presented in Table 7. One can conclude that a reasonable agreement between data and MC is obtained, in general, with the new set of JETSET parameters.
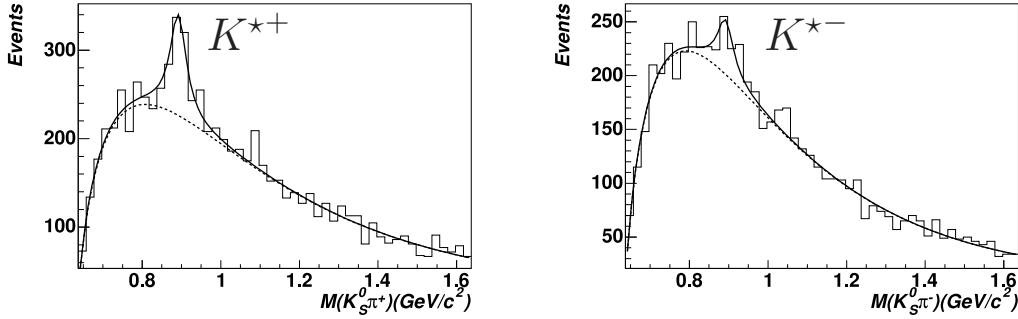

Fig. 10. $K_s^0 \pi^+$ (left) and $K_s^0 \pi^-$ (right) invariant mass distributions in the data.

Table 6
$K^{\star\pm} \to K_s^0 \pi^\pm$ summary in NC events. The fraction $f_{K^\star}$ is defined in the text. The errors are statistical only.

$K^\star$ type	Entries	$f_{K^\star}$, (%)	$f_{K^\star DATA}/f_{K^\star MC}$
$K^{\star+}$	526 ± 72	14 ± 2	1.1 ± 0.2
$K^{\star-}$	246 ± 67	6 ± 2	0.7 ± 0.2

5 Measurement of the Λ polarization

Measurement of the Λ polarization in ν NC interactions can provide some additional information with respect to the results obtained for ν_μ CC events since NC interactions are different at the quark level [17,4].
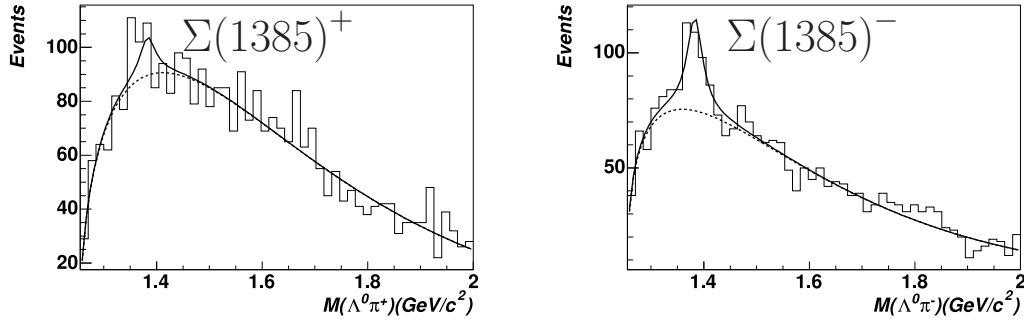
Fig. 11. $\Lambda\pi^+$ *(left) and* $\Lambda\pi^-$ *(right) invariant mass distributions in the data.*

Table 7
$\Sigma(1385)^\pm \rightarrow \Lambda\pi^\pm$ *summary in NC events. The fraction* $f_{\Sigma^\star}$ *is defined in the text. The errors are statistical only.*

$\Sigma(1385)$ type	Entries	$f_{\Sigma^\star}$, (%)	$f_{\Sigma^\star DATA}/f_{\Sigma^\star MC}$
$\Sigma(1385)^+$	47 ± 34	2 ± 2	0.5 ± 0.3
$\Sigma(1385)^-$	125 ± 32	6 ± 2	1.4 ± 0.4

The Λ polarization is measured by the *asymmetry* in the angular distribution of the protons in the parity violating decay process $\Lambda \rightarrow p\pi^-$. In the Λ rest frame the decay protons are distributed as:

$$\frac{1}{N}\frac{dN}{d\Omega} = \frac{1}{4\pi}(1 + \alpha_\Lambda \mathbf{P} \cdot \mathbf{k}), \qquad (4)$$

where $\mathbf{P}$ is the Λ polarization vector, $\alpha_\Lambda = 0.642 \pm 0.013$ [16] is the decay asymmetry parameter and $\mathbf{k}$ is the unit vector along the decay proton direction.

Since it is not possible to reconstruct the Z^0 direction in neutral current events as distinct from the W direction in the charged current events one has to redefine the coordinate system for the polarization measurement compared to the CC case [2]. For the polarization measurements in the NC sample we have chosen the coordinate system in the laboratory rest frame which is Lorentz invariant with respect to a shift along the V^0 velocity as follows:

- the $\boldsymbol{n}_x$ axis is chosen along the reconstructed V^0 direction ($\boldsymbol{e}_{V^0}$);
- the $\boldsymbol{n}_y$ axis is defined as:
  $\boldsymbol{n}_y = \boldsymbol{e}_{V^0} \times \boldsymbol{e}_\nu$, where $\boldsymbol{e}_\nu$ is the unit vector along the incoming neutrino direction.
- the $\boldsymbol{n}_z$ axis is chosen to form a right-handed coordinate system:
  $\boldsymbol{n}_z = \boldsymbol{n}_x \times \boldsymbol{n}_y$.

16

For the polarization measurements we have used the 3D method developed for the CC sample and described in detail in [2].

The Λ results are summarized in Table 8. We observe a negative polarization along the V^0 direction and in the direction orthogonal to the (ν, V^0) plane. Qualitatively these results are consistent with the longitudinal and transverse Λ polarization observed in ν_μ CC interactions [2]. The results for the $\bar{\Lambda}$ case are inconclusive because of the large statistical errors.

Table 8
The Λ polarization in NC interactions. Both statistical and systematic errors are shown.

P_x	P_y	P_z
$-0.23 \pm 0.08 \pm 0.05$	$-0.19 \pm 0.07 \pm 0.04$	$0.01 \pm 0.07 \pm 0.03$

To check the stability of the results we examined the following sources of systematic uncertainties:

- dependence of final results on the selection criteria of V^0's which include possible effects related to the contamination from fake Λ and secondary interactions. These selection criteria were varied as described in Ref. [2].
- dependence of final results on the neutral current selection criteria. The $\ln \lambda_6^{\mathrm{NC}}$ cut was varied in the interval from 0 to 1.

For each of these sources of uncertainties the maximum deviation from the reference result was found. These were then added in quadrature to give the total systematic uncertainty.

As a cross-check we measured the polarization vector of K_s^0 mesons setting the decay asymmetry parameter α to 1 and found no significant fake asymmetry (see Table 9).

Table 9
The K_s^0 "polarization" in NC interactions. Both statistical and systematic errors are shown.

P_x	P_y	P_z
$-0.03 \pm 0.03 \pm 0.01$	$-0.01 \pm 0.03 \pm 0.01$	$-0.01 \pm 0.03 \pm 0.03$

The results on the Λ polarization are compared to the phenomenological predictions within the framework of the intrinsic polarized strangeness model [4]. This is the only model currently available which can be applied to the whole x_F range. Other models [17,18] are valid only in the $x_F > 0$ interval.

In Fig. 12 we display the z dependence of the longitudinal Λ polarization measured by NOMAD and predicted by the model [4] (with the cut $E_{jet} > 3$

GeV). While the coordinate system of the model [4] is slightly different from that chosen by us (the x-axis in [4] is along the Z boson direction) we expect the angle between these two coordinate systems to be rather small.

The predictions are made for two extreme schemes: in the first scheme (model A) the Λ hyperon contains either the outgoing quark or the spectator diquark system; in the second scheme (model B) the Λ hyperon is associated with the fragmentation of either the outgoing quark or the spectator diquark depending on their phase space distance to the Λ. One can conclude that within statistical errors both models are in reasonable agreement with our data. It is important to note that the model is tuned to the Λ polarization measurements performed by NOMAD in the ν_μ CC sample, which are sensitive only to the $d - s$ quark spin correlations. The measurements from NC interactions suggest that the $d - s$ and $u - s$ spin correlations are similar.
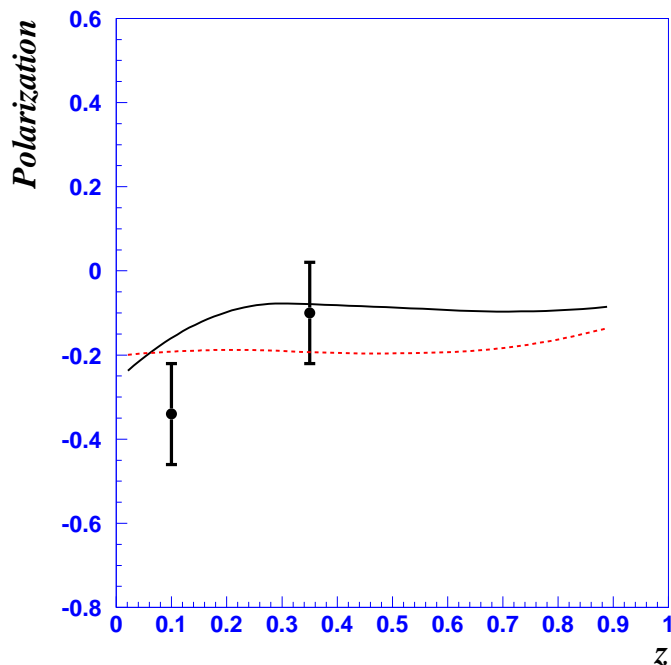

Fig. 12. The Λ polarization as a function of z measured in NOMAD compared to the intrinsic polarized strangeness model [4] predictions. Solid and dashed curves correspond to two different schemes considered in the paper [4] and named A and B, respectively (see text).

6   Conclusion

In this article we presented the results of our study of strange hadrons produced in neutrino neutral current interactions using the data from the NO-

MAD experiment. We applied an algorithm based on the event kinematics to reduce the charged current contamination in the NC sample. The background in the final sample is estimated to be about 8% of which 6% correspond to ν_μ CC contribution and the remaining 2% originate from $\bar{\nu}_\mu, \nu_e, \bar{\nu}_e$ CC contributions.

To identify neutral strange hadrons we applied the V^0 identification procedure based on a kinematic fit. As a result we found very clean V^0 samples with a background contamination of the same order as in ν_μ CC data. In 226681 identified NC interactions we have observed 3691 K_s^0's, 1619 Λ's and 146 $\bar{\Lambda}$'s about 60 times more than previously published results [1]. Integral yields of neutral strange particles have been measured to be: $(5.16 \pm 0.14(stat.) \pm 0.09(syst.))\%$, $(0.43 \pm 0.04(stat.) \pm 0.03(syst.))\%$, $(8.62 \pm 0.15(stat.) \pm 0.11(syst.))\%$ for Λ, $\bar{\Lambda}$ and K_s^0 respectively. These yields agree within few % with those measured in CC interactions. As observed by the E632 collaboration [1] at higher average neutrino energies the yields of both K_s^0 and Λ are comparable in NC and CC interactions.

Reasonable agreement has been obtained for the z distribution of neutral strange particles between the data and the predictions from a MC simulation tuned on the CC sample.

Decays of resonances and heavy hyperons with identified K_s^0 and Λ in the final state have been analyzed as well. Clear signals corresponding to $K^{\star\pm}$ and $\Sigma(1385)^{\pm}$ have been observed.

First results on the measurements of the Λ polarization in neutrino neutral current interactions are presented. The results are close to those observed in ν_μ CC interactions with a somewhat larger statistical uncertainty. The results for the longitudinal polarization of Λ hyperons are in agreement with the predictions of the intrinsic polarized strangeness model [4].

Acknowledgements

References

[1] M. Aderholz *et al.*, [E-632 Collaboration], Phys. Rev. D **45** (1992) 2232.

[2] P. Astier *et al.*, [NOMAD Collaboration], Nucl. Phys. B **588** (2000) 3.

[3] P. Astier *et al.*, [NOMAD Collaboration], Nucl. Phys. B **605** (2001) 3.

[4] J. R. Ellis, A. Kotzinian and D. V. Naumov, Eur. Phys. J. C **25** (2002) 603, [hep-ph/0204206].

[5] J. Altegoer *et al.* [NOMAD Collaboration], Nucl. Instr. Meth. A **404** (1998) 96.

[6] M. Anfreville *et al.*, Nucl. Instr. and Meth. A **481** (2002) 339.

[7] G. Bassompierre *et al.*, Nucl. Instr. and Meth. A **403** (1998) 363;
G. Bassompierre *et al.*, Nucl. Instr. and Meth. A **411** (1998) 63.

[8] D. Autiero *et al.*, Nucl. Instr. and Meth. A **373** (1996) 358;
D. Autiero *et al.*, Nucl. Instr. and Meth. A **387** (1997) 352;
D. Autiero *et al.*, Nucl. Instr. and Meth. A **411** (1998) 285.

[9] P. Astier *et al.* [NOMAD Collaboration], Nucl. Instr. Meth. A **515** (2003) 800.

[10] G. Ingelman, LEPTO version 6.1, "The Lund Monte Carlo for Deep Inelastic Lepton-Nucleon Scattering", TSL-ISV-92-0065 (1992);
G. Ingelman, A. Edin, J. Rathsman, LEPTO version 6.5, Comp. Phys. Comm. **101** (1997) 108, [hep-ph/9605286].

[11] T. Sjöstrand, "PYTHIA 5.7 and JETSET 7.4: physics and manual", LU-TP-95-20 (1995), [hep-ph/9508391];
T. Sjöstrand, Comp. Phys. Comm **39** (1986) 347, **43** (1987) 367.

[12] GEANT : Detector Description and Simulation Tool, *CERN Programming Library Long Writeup* **W5013**, GEANT version 3.21.

[13] P. Astier *et al.*, [NOMAD Collaboration], Nucl. Phys. B **621** (2001) 3.

[14] S.I. Alekhin, Phys. Rev. D **68** (2003) 014002.

[15] P. Astier *et al.* [NOMAD Collaboration], Nucl. Phys. B **611** (2001) 3.

[16] Review of Particle Properties, Phys. Rev. D **66** (2002) 010001.

[17] M. L. Mangano *et al.*, "Physics at the front-end of a neutrino factory: A quantitative appraisal", CERN-TH/2001-131, [hep-ph/0105155];
A. Blondel *et al.*, "ECFA/CERN studies of a European neutrino factory complex," CERN-2004-002.

[18] M. Anselmino, M. Boglione, U. D'Alesio and F. Murgia, Eur. Phys. J. C **21** (2001) 501, [hep-ph/0106055].